A novel methodology for the evaluation of low temperature failure properties of asphalt binders

A novel methodology for the evaluation of low temperature failure properties of asphalt binders

Orazio Baglieri, Chiara Tozzi, Davide Dalmazzo, Lucia Tsantilis, Ezio Santagata*
Department of Land, Environment and Infrastructure Engineering, Politecnico di Torino, Torino, Italy

(*) corresponding author: ezio.santagata@polito.it

Abstract. This paper presents the results of an experimental investigation that focused on the failure properties of asphalt binders at low temperatures. A novel test method was developed, based on the use of the dynamic shear rheometer equipped with 4 mm parallel plates. The method entails the application of constant shear strain rates at various temperatures until failure. Test data are modelled by means of the elastic-viscoelastic correspondence principle and by thereafter referring to the shear stress at failure, to a purposely defined brittleness index and to a critical brittleness temperature. Results discussed in the paper, which refer to a preliminary set of experimental data, indicate that the proposed methodology may be very effective in evaluating and comparing low temperature failure properties of asphalt binders of various types and origins.

Keywords: asphalt binder; low temperature properties; dynamic shear rheometer; elastic-viscoelastic correspondence principle; brittleness index

1 Introduction

Thermal cracking represents one of the main distresses affecting asphalt pavements. This distress typically occurs in cold regions in the form of regularly spaced transverse cracks caused by thermally induced stresses that exceed the tensile strength of asphalt mixtures. The cracking mechanism taking place within the pavement depends upon several factors that are material-, structure-, and environment-related [1-2]. In particular, it has been widely recognized that the low temperature properties of the asphalt binder play a key role in controlling crack initiation and propagation phenomena [3-5].

Over the past decades, various test methods have been proposed for low temperature characterization of asphalt binders. With different levels of reliability, they have been all used for the purpose of selecting and comparing these materials with respect to their potential resistance to thermal cracking.

The standardized method that has been employed for the longest time by asphalt technologists for low temperature characterization consists in the determination of the Fraass breaking point [6]. Such a parameter provides a measure of the brittleness of a thin film of asphalt binder subjected to a predefined cooling rate. Due to the empirical nature of

this test procedure, obtained experimental results are affected by a low level of precision and accuracy. Moreover, Fraass breaking point shows a poor correlation with the field behaviour of asphalt mixtures and for this reason its use as a low temperature performance indicator is not highly recommended [7].

Other more recent and scientifically sound standardized methods are those that refer to flexural tests performed by means of the Bending Beam Rheometer (BBR) [8] and to uniaxial tension tests carried out by means of the Direct Tension Tester (DTT) [9]. Creep stiffness and creep rate derived from BBR tests are usually sufficient for determining the so-called low-temperature performance grade (PG) of asphalt binders (also indicated as low limiting PG temperature) [10]; however, axial strain at failure coming from DTT tests can also be employed for such a purpose when considering stiff binders characterized by a significant ductility [11-12]. BBR and DTT test methods have also been used beyond the PG grading system as part of research projects focused on various aspects of low temperature cracking, including the effects of binder source and polymer modification [13-14], the behaviour of mastics and mortars [15-17], and the occurrence of physical hardening [18-20]. Notwithstanding the merits of both test methods, several studies have highlighted some of their limits. In particular, it has been shown that binders with the same low limiting PG temperature may exhibit significant differences in terms of actual performance in the field [21-22], and that use of such a limiting temperature may not be effective in capturing the enhanced low temperature performance of polymer-modified bitumen (PMB) [23]. In the case of BBR tests, the main shortcomings derive from the fact that loading conditions do not lead to the rupture of test specimens, thereby preventing any direct assessment of the tensile strength and cracking resistance of the material. From the comparison of binder creep data with mixture creep data, other researchers concluded that the BBR test should not be used to predict thermal stresses in asphalt pavements [24]. Moreover, BBR tests require the use of a relatively high amount of material and this can be a significant limit when investigating low temperature properties of binders recovered from an existing pavement [25].

As an alternative to BBR and DTT tests, recent development work has led to the proposal of test methods for the characterization of low temperature properties of asphalt binders based on the use of the Dynamic Shear Rheometer (DSR) [26-29]. Experimental challenges of such an approach are related to the effects of instrument compliance, that can generate significant errors in the evaluation of the absolute values of the dynamic and relaxation moduli. To overcome this problem, proposed test protocols require 4 mm parallel plates to be employed for testing and raw data to be corrected following the procedure adopted by Schröter [30]. The 4 mm plate geometry was successfully employed by Lu et al. [25] when comparing DSR test data collected at temperatures as low as -30 °C to the results obtained

from BBR tests. Riccardi et al. [31] found a relationship linking creep stiffness and creep rate determined with the BBR to the relaxation modulus and creep rate obtained from DSR tests, concluding that low limiting PG temperature obtained from the two types of measurement are equivalent. Wang et al. [32] focused on the results of DSR tests carried out on various asphalt binders by using 4 mm parallel plates and different measurement gaps. Based on the evaluation of master curves and related fitting models, they observed that similar rheological properties were obtained with all considered gaps. Although the outcomes of the abovementioned studies provided valuable information on the low temperature characterization of asphalt binders, it should be emphasized that they entailed the use of the DSR for the evaluation of viscoelastic properties at relatively small strain amplitudes, under testing conditions in which the response of the materials is expected to be linear and far from failure.

The research work presented in this paper focused on the low temperature behaviour of asphalt binders in the high strain domain, with the purpose of highlighting non-linear effects and investigating the mechanisms that ultimately lead to failure in torsion. As illustrated in the following sections, laboratory tests were carried out with the DSR by subjecting slender cylindrical specimens to monotonic torsional loading at various temperatures and strain rates. Experimental data obtained from this novel test method were analysed by making use of the elastic-viscoelastic correspondence principle [33] and by thereafter referring to appropriate strength and brittleness parameters. Experiments were conducted on a set of neat binders of various types and origins with the purpose of assessing the effectiveness of this methodology in discriminating the low temperature properties of different materials.

2 Materials

Three neat asphalt binders (labelled as A, B and C) were used in the experimental study. They were provided by refineries which operate on crudes of various origins and differed in terms of penetration grade as indicated in the following: 40/60 (binder A), 50/70 (binder B), and 70/100 (binder C).

In order to highlight the role played by the physicochemical nature of materials, each binder was subjected to a preliminary laboratory investigation which included fractionation analysis, linear viscoelastic characterization, and determination of glass transition temperature.

2.1 Fractionation analysis

Information on the chemical composition and structure of asphalt binders was gathered from fractionation analysis carried out by employing a technique that combines Thin Layer Chromatography (TLC) and Flame Ionization Detection (FID) [34-36]. TLC allows the

separation of saturates, aromatics, resins and asphaltenes (also known as SARA fractions) through their successive elution in solvents of increasing polarity (n-hexane, toluene and a solution of dichloromethane and methanol in a volume ratio of 95:5), while FID yields the relative amounts of each of the four abovementioned fractions.

Based on the results of fractionation analysis, the internal structure of bitumen can be represented in simplified terms as a colloidal system [37], in which agglomerations of asphaltenes are dispersed in a continuous phase composed by aromatics and saturates, with resins acting as anti-flocculating agents. It has been demonstrated that asphaltenes affect strength and stiffness of the material, resins provide adhesion and ductility, while aromatics and saturates influence viscosity [38]. Saturates, which contain paraffins, also promote the development of physical hardening phenomena at low temperatures [39-40]. The colloidal stability of asphalt, which encompasses the possible transition from a sol-type to a gel-type structure, can be evaluated by referring to the Gaestel index (I_C, also known as index of colloidal instability), calculated as the ratio of the cumulative percentages of asphaltenes and saturates to the sum of the percentages of aromatics and resins [41]. Results obtained from the above described fractionation analysis, performed by means of a Iatroscan MK-6 analyser, are reported in Table 1.

Table 1 SARA fractions and Gaestel index of asphalt binders

Binder	Saturates (%)	Aromatics (%)	Resins (%)	Asphaltenes (%)	I_C (-)
A	5.1	45.4	18.7	30. 8	0.56
B	6.3	39.8	29.7	24. 2	0.44
C	6.1	44.1	22.8	26.9	0.49

The data shown in Table 1 clearly reflect the different origin and source of the considered asphalt binders. In fact, despite the similarity in saturates content, percentages corresponding to aromatics, resins and asphaltenes varied significantly. In particular, it was observed that the relative amount of resins was lower than that of asphaltenes in the case of binders A and C (40/60 and 70/100, respectively), while resins exceeded asphaltenes in the case of binder B (50/70). Differences were also observed when referring to the I_C parameter, with binder A showing the highest value (equal to 0.56), followed by binder C (0.49) and binder B (0.44). Based on these data, the colloidal structure of all investigated materials was considered to be stable [42], the densest gel-like structure being hypothesised for binder A.

2.2 Linear viscoelastic characterization

The linear viscoelastic properties of the asphalt binders were evaluated by means of frequency sweep tests performed at multiple temperatures by following a procedure similar to that described in AASHTO T315-2012 [43]. In particular, measurements were carried out by making use of an AntonPaar MCR302 DSR equipped with 4 mm, 8 mm and 25 mm parallel plates, at test temperatures varying from -25 °C to 76 °C and at frequencies ranging between 1 rad/s and 100 rad/s for each temperature. Strains applied at individual temperature-frequency combinations were conveniently varied in order to operate within the linear viscoelastic domain.

Fig. 1 shows test results represented in the form of the so-called Black diagram, in which the norm of the complex modulus ($|G^*|$) is plotted as a function of phase angle (δ). This type of representation of test results is usually employed to identify inconsistencies in rheological measurements and to verify the validity of the time-temperature superposition principle [44].

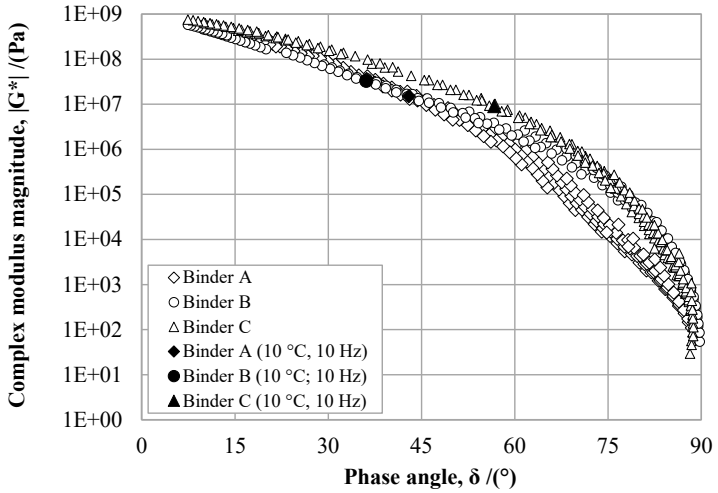

Fig. 1 Black diagrams of asphalt binders

It was observed that curves corresponding to asphalt binders B and C (50/70 and 70/100, respectively) were continuous, thereby indicating that these materials can be considered as rheologically simple. Consequently, the time-temperature superposition principle could be applied over the entire range of investigated temperatures and frequencies to construct master curves and model viscoelastic behaviour. In the case of asphalt binder A (40/60), it was noticed that the Black curve was characterized by a continuous trend only for phase angle values up to 45°, above which data sets collected at different temperatures became disjointed and scattered. Such an outcome can be related to the high amount of asphaltenes of this material, thereby suggesting that the presence of a dense gel-like internal structure can lead to a complex rheological behaviour [44-45]. It follows that in the case of binder

A, the time-temperature superposition principle was considered to be valid at low temperatures only.

With the purpose of comparing the response of the three asphalt binders in the same testing conditions, data points corresponding to the reference temperature of 10 °C and to the reference frequency of 10 rad/s are highlighted on the Black diagrams of Fig. 1. It was observed that binder C (70/100) showed the highest value of δ and the lowest value of $|G^*|$, followed by binders A and B. This order is not fully coherent with the penetration grades of the considered binders, according to which binder A (40/60) is characterized by a higher level of hardness with respect to binder B (50/70).

2.3 Determination of glass transition temperature

Glass transition is a phenomenon that affects the low temperature properties of amorphous materials. It is defined as a reversible change from a viscous to a hard and relatively brittle glassy state, accompanied by a sudden change in the thermodynamic and mechanical properties. In the case of asphalt binders, glass transition does not occur abruptly since the material is composed of several fractions that have different glass transition points. Therefore, the glass transition temperature (T_g) cannot be identified in a univocal way and is arbitrarily chosen as the temperature that represents the range over which the overall glass transition phenomena take place [46].

No standard methods are currently available for determining the T_g of asphalt binders. The various techniques that have been proposed by researchers are based, depending upon the case, on dilatometric analyses, differential scanning calorimetry and rheological measurements [47]. The technique adopted for the evaluation of the T_g of the binders considered in this study is based on the representation of the peak value of loss modulus (G") versus temperature (T). For such a purpose, the Christensen-Anderson model [48] was fitted to data gathered from linear viscoelastic characterization tests over the interval comprised between -25 °C and 0 °C. Subsequently, T-G" curves were derived from fitted data at a reference frequency of 1 Hz.

Results obtained from the above described analysis are reported in Table 2. It was found that binder B (50/70) had the highest T_g value followed, in the order, by binder C (70/100) and binder A (40/60). Table 2 also contains the values of a thermal susceptibility parameter, calculated as the average slope of the $\log(|G^*|)$ versus T curve in two non-overlapping temperature intervals: the first one ranging from 0 °C to T_g and the second one ranging from T_g to -35 °C. These two intervals were selected by considering that sensitivity to temperature variations is expected to change significantly above and below the glass transition point. Experimental data confirmed such an expectation, showing that thermal susceptibility is significantly reduced when passing from the first (higher) to the second (lower) temperature interval. Binder B (50/70) showed lower susceptibilities with respect

to the other two binders, while binder A (40/60) was found to be less sensitive to temperature changes than binder C (70/100).

Table 2 Glass transition temperature and thermal susceptibility parameters of asphalt binders

Binder	T_g [°C]	Thermal susceptibility	
		0 °C to T_g	T_g to -35 °C
A	-23.2	0.038	0.016
B	-13.4	0.028	0.013
C	-16.2	0.051	0.017

3 Evaluation of low temperature failure properties

3.1 Test procedure and specimen preparation

The methodology developed to evaluate low temperature failure properties of asphalt binders is based on the use of the DSR equipped with 4 mm parallel plates. The test procedure includes three subsequent phases.

The first phase consists in the thermal conditioning of the test specimen. Adequate control of temperature during this phase represents a critical factor affecting the accuracy and repeatability of the results, due to the possible build-up of tensile stresses and to the potential occurrence of hardening phenomena. Based on various preliminary attempts aimed at preventing the abovementioned undesired effects, the conditioning process was divided in three steps:

- Step I - temperature is gradually reduced from a fixed initial value of 20 °C to an intermediate value of 4 °C by imposing a cooling rate of 2 °C/min;
- Step II - temperature is decreased from 4 °C to the target test temperature by imposing a cooling rate of 1 °C/min;
- Step III - the specimen is allowed to rest for 45 min in order to achieve thermal equilibrium.

The gap between the parallel plates is automatically reduced during the cooling process in order to maintain the normal force close to zero and to avoid the possible creation of internal stresses caused by volume change.

The second phase of the test procedure consists in a fingerprinting test, entailing a frequency sweep performed at the test temperature in the range between 1 rad/s and 100 rad/s with an applied shear strain amplitude of 0.05 %. Results obtained from this test are used in data analysis to account for specimen-to-specimen variability.

The third phase of the procedure consists in a monotonic torsional loading (MTL) test carried out at constant temperature and shear strain rate until failure.

Temperatures imposed during MTL tests carried out on the three asphalt binders (A, B and C) varied from -25 °C to -5 °C with 5 °C increments. Two strain rates, equal to 0.0005 s^{-1} and 0.001 s^{-1}, were adopted at each temperature. These strain rates were defined based on the results of explorative tests in order to remain within the instrument limits and to produce a brittle fracture.

In order to reduce specimen torsional stiffness, the gap between plates was set equal to 5 mm. However, such a choice posed some experimental challenges. Firstly, this unusual specimen thickness did not allow the DSR conditioning hood to be completed lowered, thus causing the presence of a gap between its lower surface and the upper surface of the measuring device base. To overcome this problem and to avoid heat dispersions, a polystyrene disk was used to fill the abovementioned gap. Secondly, significant efforts were made to find an easy and repeatable way to prepare test specimens. After a series of trials, the following procedure was used: i) the gap between plates is zeroed, and the upper 4 mm plate is released and fitted with a mould made by rolling an aluminium sheet , ii) a small amount (around 0.1 g) of asphalt binder is inserted into the mould and thereafter heated in order to ensure good adhesion between the material and the plate, iii) the mould filled with the binder is placed in a refrigerator for 15 min, in order to easily remove the aluminium sheet without causing any damage to the specimen, iv) the specimen is cut by means of a hot spatula to obtain the target height of 5 mm, v) the upper plate is placed back into the instrument and lowered until the end surface of the cylindrical specimen comes in contact with the pre-heated lower plate of the DSR, vi) target measurement gap is imposed between the parallel plates.

3.2 Assessment of machine compliance

The concept of instrument (or machine) compliance stems from the consideration that the deflection angle recorded in torsion by the DSR (φ_m) is given by the deformation of the specimen being tested (φ_s) and the deformation of the measuring tool (φ_t), according to the following equation:

$$\varphi_m = \varphi_s + \varphi_t = \frac{M}{K_s} + \frac{M}{K_t} \quad (1)$$

where M is the applied torque [N·m], K_s is the torsional stiffness of the specimen [N·m/rad], and K_t is the torsional stiffness of the instrument [N·m/rad].

Under testing conditions in which the value of K_s is significantly lower than that of K_t, the second term on the right-hand side of Eq. (1) (i.e. φ_t) is negligible. In the specific case of asphalt binders, this assumption is valid at sufficiently high temperatures (> 5 °C) [27]. Conversely, at lower temperatures the stiffness of the specimen is comparable to the

stiffness of the instrument and as a consequence, the deformation of the instrument φ_t can no longer be neglected. Thus, machine compliance (J_t), defined as the inverse of K_t, needs to be determined to correct test data [49].

For the DSR measurements performed during the experimental investigation described in this paper, J_t was assessed by measuring the deformations exhibited by parallel plates "glued" together with a very thin film of asphalt binder (0.05 mm thickness) at a very low temperature (-35 °C). Measurements were carried out by means of two different techniques: a torque sweep oscillatory test at a frequency of 1 rad/s, and a monotonic torque test with an imposed linear rate of torque increment equal to 20 mN·m/min. Deflection angles gathered from these tests were plotted as a function of the applied torque and J_t was then calculated as the slope of linear fits. This is displayed in Fig. 2, which also shows the obtained fitting equations.

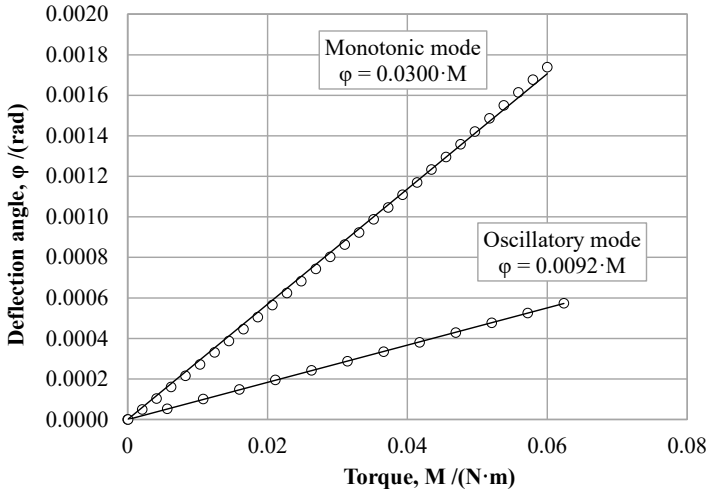

Fig. 2 Deflection angle as a function of applied torque (for assessment of machine compliance)

As indicated in Fig. 2, the two adopted techniques led to different J_t values, the one obtained in the continuous mode (equal to 0.03 rad/N/m) being higher than the one obtained in the oscillatory mode (equal to 0.0092 rad/N/m). Calculated J_t values were then used to adjust the device settings for the automatic correction of data measured during the two types of test (oscillatory or monotonic). However, it was discovered that the controlling software of the employed DSR has a real-time instrument compliance correction function for the oscillatory mode only. Hence, in the case of monotonic tests, corrections were manually made by using the following equation:

$$\varphi_s = \varphi_m - J_t \cdot M \quad (2)$$

with J_t equal to 0.03 rad/N/m.

4 Results and discussion

4.1 Stress-strain data

Fig. 3 shows an example of experimental results obtained from MTL tests, represented in terms of shear stress (τ) as a function of shear strain (γ). Coherently with expectations, it was observed that the response of tested materials changed significantly with test temperature and/or shear strain rate. In fact, stress-strain curves showed a tangent slope that progressively decreased with the increase of strain level, the variation being more pronounced at higher temperatures and lower strain rates. Such an occurrence, which is commonly described as a non-linear effect, was analysed in detail as illustrated in section 4.2 of this paper.

(a)

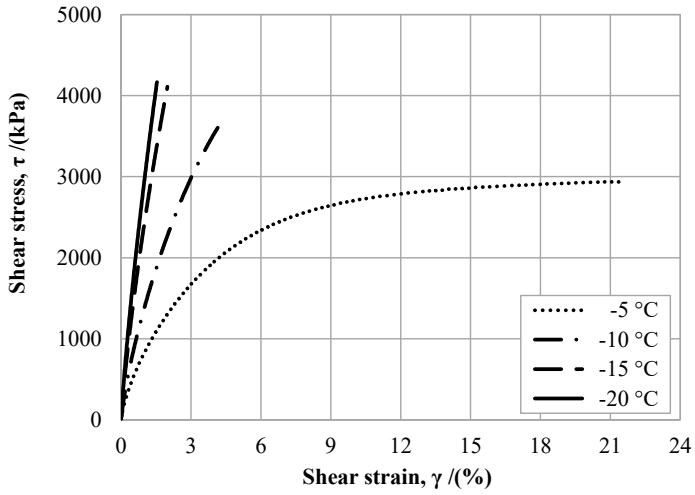

(b)

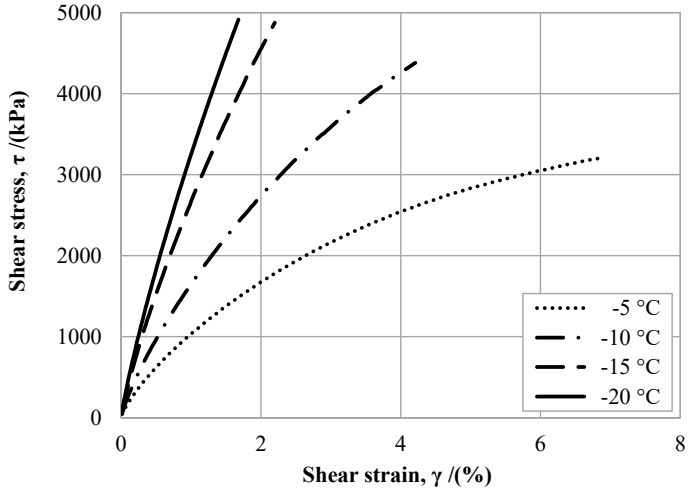

Fig. 3 Stress-strain curves at various temperatures obtained for binder B at two different strain rates: (a) 0.0005 s^{-1}, (b) 0.001 s^{-1}

In general terms, failure of a cylindrical specimen under torsional loading may occur, depending upon the characteristics of the material, along the axial shear plane or along a plane with an inclination of ±45° (Fig. 4). The first type of failure mechanism is typically associated to a ductile-like response, while the second one is more frequent in the case of a brittle-like behaviour [50].

In the case of the considered asphalt binders, the type of failure reached at the end of MTL tests was identified by visually examining the morphology of failure surfaces. As indicated in Table 3, the occurrence of a ductile-like or brittle-like failure depended on the combination of temperature and shear strain rate used for testing. However, only experimental tests which led to a brittle-like failure of specimens were considered for data analysis, since more relevant for the scope of the study. It should also be mentioned that in brittle-like failure conditions the breaking point of a specimen can be clearly identified, thus allowing the straightforward determination of corresponding shear strain and shear stress terminal values.

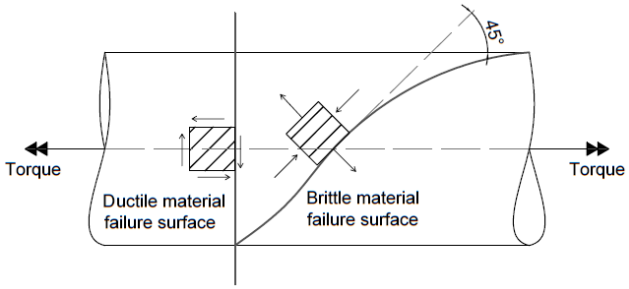

Fig. 4 Schematic illustration of ductile and brittle failure surfaces (adapted from [51])

Table 3 Type of failure mechanisms observed at various temperatures and strain rates (D = ductile-like, B = brittle-like)

Binder	Strain rate (s^{-1})	-5 °C	-10 °C	-15 °C	-20 °C	-25 °C
A	0.0005	D	D	B	B	B
	0.001	D	D	B	B	B
B	0.0005	B	B	B	B	-
	0.001	B	B	B	B	-
C	0.0005	D	D	D	B	B
	0.001	D	D	B	B	B

Shear strains (γ_{max}) and shear stresses (τ_{max}) at failure obtained for the considered asphalt binders from MTL tests carried out at various temperatures and strain rates are displayed in Fig. 5.

(a)

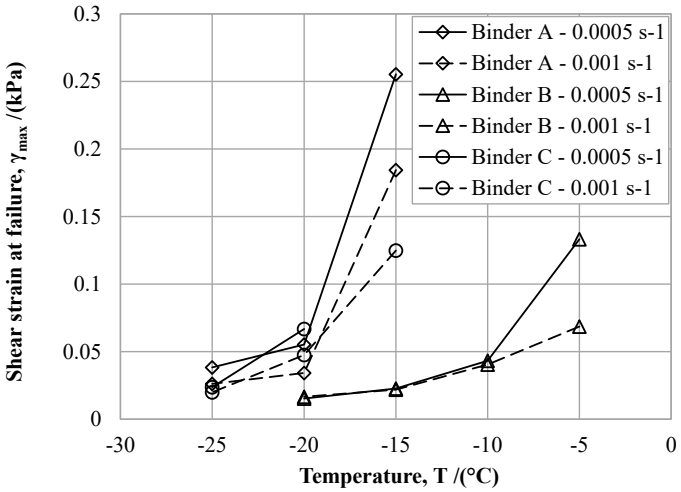

(b)

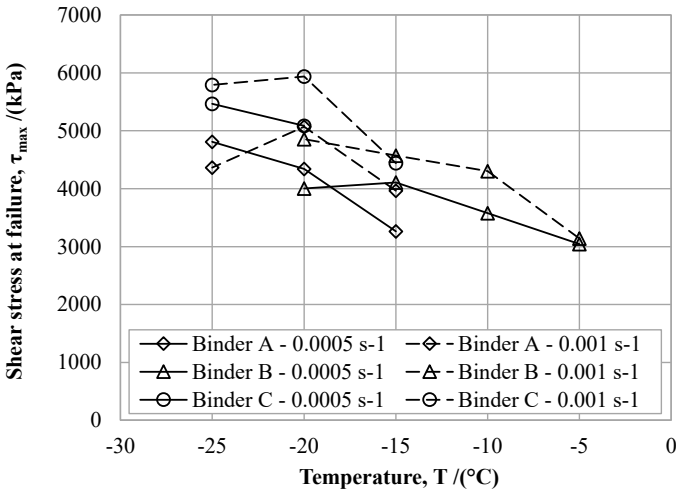

Fig. 5 Results of MTL tests: (a) strain and (b) stress at failure versus temperature at different strain rates

The diagrams shown in Fig. 5 indicate that with the decrease of temperature, stress at failure (i.e. strength) and strain at failure increased and decreased, respectively. Such an outcome is fully coherent with expectations, since asphalt binders exhibit a progressive enhancement of strength and brittleness as temperature gradually drops. Furthermore, for any given temperature, a decrease of failure strain and an increase of strength were observed when passing from the lower to the higher strain rate imposed to test specimens. This is also coherent with expectations, due to the viscoelastic nature of these materials. Finally, it was noticed that for each considered asphalt binder, T- τ_{max} curves displayed a sudden change in slope around the T_g value, with a tendency to reach a horizontal plateau when moving towards lower temperatures. The only exception to this trend was found for binder A (40/60) at the higher strain rate, probably as a consequence of specimen non-homogeneity. This general outcome suggests the existence, for each material, of a shear strength threshold

that is dependent upon strain rate and leads to almost constant strength values in the glass transition region.

Further considerations can be drawn from Fig. 5 by comparing the selected asphalt binders to each other. In particular, binders A (40/60) and C (70/100) appeared to be more sensitive to temperature variations than binder B (50/70), thus highlighting a behaviour that is consistent with their higher values of the thermal susceptibility parameters indicated in Table 2. Differences in thermal sensitivity reflected on the ranking of materials in terms of strength, that seemed to be significantly dependent upon temperature. For example, at -20 °C binder A (40/60) exhibited the highest stress at failure, followed in the order by binders C (70/100) and B (50/70). However, this ranking completely changed at -15 °C, where binder B displayed the highest shear strength among all binders. Finally, it should be underlined that binder B showed the lowest values of strain at failure in all test conditions considered in the investigation. This outcome seems to be consistent with the highest value of T_g exhibited by this binder, which in comparison to the other binders was characterized by a more extended region of glassy behaviour.

4.2 Pseudo-strains

As discussed in the previous section, γ-τ curves obtained from MTL tests are characterized by a curved shape, with deviations from the linearity that were found to be dependent upon temperature and strain rate. Although such an occurrence is commonly referred to as non-linearity, it should be underlined that it stems from the combined effects of three distinct factors: time dependency (as a result of the viscoelastic nature of the material), stress (or strain) dependency (i.e. true material non-linearity), and damage. However, in order to clearly assess the true failure behaviour of asphalt binders, it was deemed necessary to remove time effects from test results. This result was achieved by making use of the elastic-viscoelastic correspondence principle [33], that allows true strains to be transformed into pseudo-strains, as shown in the following.

By definition, pseudo-strain $\gamma^R(t)$ is given by the following expression:

$$\gamma^R(t) = \frac{\tau(t)}{G^R} \tag{3}$$

where τ(t) is the shear linear viscoelastic stress and G^R is a reference modulus, usually assumed as equal to 1.

Shear stress can be calculated by means of the convolution integral expressed by Eq. (4).

$$\tau(t) = \int_0^{t_R} G(t_R - \xi)\frac{d\gamma}{d\xi}d\xi \tag{4}$$

where G is the relaxation shear modulus, t_R is the reduced time and ξ is the time variable of integration.

By substituting Eq. (4) into Eq. (3), the pseudo-strain formula becomes:

$$\gamma^R(t) = \int_0^{t_R} G(t_R - \xi)\frac{d\gamma}{d\xi}d\xi \quad (5)$$

Solution of Eq. (5) involves determining the relaxation shear modulus functions of the considered material. For the asphalt binders included in the experimental investigation, the analytical form of these functions was expressed by referring to a Prony series formulation based on the Generalized Maxwell model, according to Eq. (6):

$$G(t) = G_\infty + \sum_{m=1}^{M} G_m \cdot e^{-t_R/\rho_m} \quad (6)$$

where G_∞ is the long-time elastic modulus (equal to zero for asphalt binders), M is the number of elements in the Prony series, G_m and ρ_m are Prony coefficients.

Combination of Eq.(6) with Eq. (5) leads to the following expression of pseudo-strain:

$$\gamma^R = \int_0^t \left(\sum_{m=1}^{M} G_m \cdot e^{-t_R/\rho_m}\right)\frac{d\gamma}{d\xi}d\xi \quad (7)$$

As a results of these analytical developments, the constitutive equations for a viscoelastic material are equivalent to the equations of an elastic material in the stress - pseudo-strain (τ-γ^R) space. Thus, pseudo-strain can be related to stress by means of Hooke's law:

$$\tau(t) = C \cdot \gamma^R \quad (8)$$

where C is pseudo-stiffness.

From Eq. (8) it follows that the γ-τ curves obtained from MLT tests carried out on asphalt binders become straight lines in the γ^R-τ space if these materials are characterized by a linear viscoelastic behaviour until failure, with no progressive cumulation of damage. Conversely, any deviation from linearity in the γ^R-τ plots indicates the progressive occurrence of the combined effects of material non-linearity and damage.

Pseudo-stiffness C was corrected with specimen-to-specimen factors given by the differences between the average linear viscoelastic behaviour corresponding to the Christensen-Anderson model and the linear viscoelastic behaviour assessed with the fingerprinting test (in the second phase of the proposed testing procedure). These specimen-to-specimen factors were found to vary between 0.9 and 1.1.

Prony coefficients G_m and ρ_m were determined from data gathered in the frequency domain by implementing a linear viscoelastic interconversion based on the following relationship derived from Fourier transformation:

$$G'(\omega_R) = \sum_{m=1}^{M} \frac{G_m \omega_R^2 \rho_m^2}{\omega_R^2 \rho_m^2 + 1} \quad (9)$$

where G' is the storage shear modulus at reduced frequency ω_R.

Calculation of pseudo-strains is very sensitive to experimental variability. Thus, only results of the frequency sweep tests at low temperature (from -25 °C to -5 °C) were considered in the analysis in order to obtain the best estimate of viscoelastic properties in the range of interest.

ρ_m and G_m coefficients were determined by means of the collocation method. In particular, ρ_m values were selected to be spaced two decades apart and angular frequencies ω_i were selected to be equal to ρ_{mi}. Coefficients G_m were then expressed as the cross product of the inverse of the relaxation kernel matrix $[B_m]$ and the shifted storage modulus array $\{G'\}$, as shown in Eq. (10):

$$G_m = [B_m]^{-1} x \{G'\} \tag{10}$$

with i-terms of the relaxation kernel matrix given by:

$$B_{mi} = \frac{\omega_i^2 \rho_{mi}^2}{\omega_i^2 \rho_{mi}^2 + 1} \tag{11}$$

Once the Prony terms were determined, the pseudo-strain convolution integral was solved via a numerical technique based on the state variable concept and on the following updating rule:

$$\psi_m{}^{n+1} = e^{-\Delta t_R/\rho_m} \psi_m^n + G_m \cdot \rho_m \left(\frac{\gamma^{n+1} - \gamma^n}{\Delta t_R} \right) \left[1 - e^{-\Delta t_R/\rho_m} \right] \tag{12}$$

where $\psi_m{}^{n+1}$ is the value of the m-th Prony term state variable at the n+1 time step, ψ_m^n is the value of the m-th Prony term state variable at the n time step, t_R is reduced time, γ^{n+1} is physical strain at the n+1-time step; γ^n is physical strain at the n time step.

Pseudo-strain at the n+1-time step was finally assessed by summing all the m state variables, as per Eq.(13):

$$\gamma^{R\,n+1} = \sum_{m=1}^{N} \psi_m{}^{n+1} \tag{13}$$

An example of MTL test results diagrammed in the stress - pseudo-strain domain is shown in Fig. 6, which also displays the space bisector that corresponds to the behaviour of a perfectly linear viscoelastic material. For the considered binder (B), it was observed that as temperature was decreased, τ-γ^R curves gradually tend to approach the bisector, thus indicating that the response of the material becomes almost linear viscoelastic until failure. The same tendency was observed for the other asphalt binders (A and C) at both strain rates.

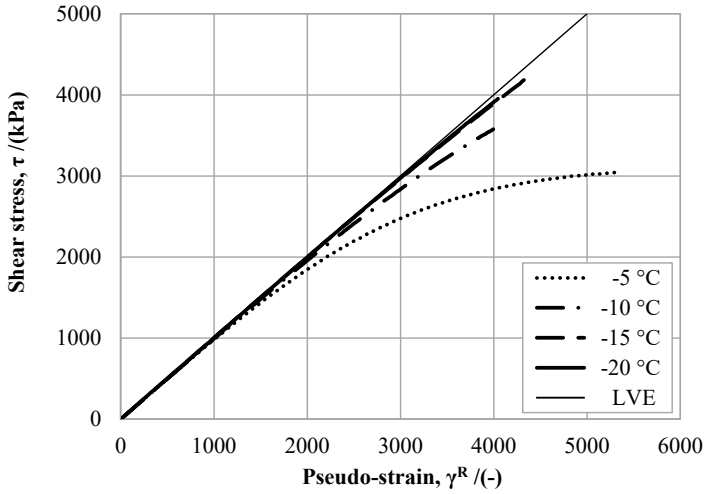

Fig. 6 Shear stress versus pseudo-strain at various temperatures for binder B (strain rate equal to 0.0005 s^{-1})

4.3 Pseudo-strain energy density and brittleness

As discussed in the previous section, pseudo-strain - stress curves obtained from MTL tests provide relevant information on the possible occurrence of non-linear and damage effects during the entire loading process until failure. However, a full assessment of the low temperature behaviour of the asphalt binders also requires the evaluation of their toughness, which can be quantified by calculating the energy per unit volume (i.e. energy density) they absorb before rupturing. Such a characteristic is meaningful with respect to performance and can ultimately be considered in the process of selecting asphalt binders. Since asphalt binders are viscoelastic in nature, rather than considering physical energy density, it is necessary to refer to pseudo-strain energy density as defined in the following.

Two different values of pseudo-strain energy density were determined from MTL test data plotted in the stress - pseudo-strain diagram. The first one, referred to as the effective pseudo-strain energy density (w^R), was calculated as the area under the stress - pseudo-strain curves until failure according to Eq. (14):

$$w^R = \int \tau(t)\, d\gamma^R \tag{14}$$

The second one, referred to as potential pseudo-strain energy density (w^R_{LVE}), was calculated as the area under the linear viscoelastic line by Eq. (15):

$$w^R_{LVE} = \int \tau_{LVE}(t)\, d\gamma^R \tag{15}$$

w^R represents the amount of pseudo-strain energy per unit volume actually involved in the material deformation process, while w^R_{LVE} represents the maximum energy per unit volume corresponding to the undamaged and linear viscoelastic response. The limit case for which w^R is equal to w^R_{LVE} refers to specific conditions in which asphalt binders exhibit a linear

viscoelastic behaviour until failure, with rupture occurring abruptly. By analogy with the elastic case, this type of behaviour can be considered as perfectly brittle.

In order to quantitively assess the brittleness of the considered asphalt binders, a brittleness index (I_B) was defined according to Eq. (16):

$$I_B = \frac{w^R}{w^R_{LVE}} \tag{16}$$

Values of I_B calculated at different temperatures and strain rates are reported in Fig. 7. As expected, brittleness of all binders increased with the decrease of temperature and/or with the increase of imposed strain rate. Moreover, in most cases the experimental temperature - I_B curves displayed a common trend characterized by a slope that gradually decreased when approaching the limiting I_B value of 1 (that corresponds to a purely brittle behaviour). It was also noticed that the various binders reached these purely brittle limiting conditions at temperatures that were rather different from each other.

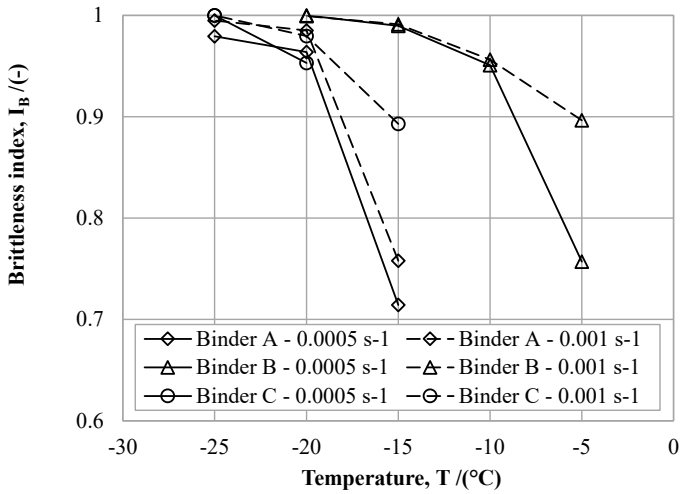

Fig. 7 Brittleness index of asphalt binders

For comparison purposes, a critical brittleness temperature (T_{cr}) corresponding to a conventional threshold of I_B equal to 0.98 was determined for each binder at both strain rates. Values of T_{cr}, obtained by linear interpolation between pairs of data points located immediately above and below the threshold, are reported in Table 4. For each binder it was found that T_{cr} increased with the increase of applied strain rate. This is coherent with expectations since a strain rate increment emphasizes the elastic and brittle components of response, and materials consequently reach their critical conditions at higher temperatures. It was observed that binder B showed T_{cr} values which were significantly higher than those exhibited by the other two binders (A and C). This finding is consistent with the ranking associated to binder B in terms of its glass transition temperature T_g (Table 2) and suggests

that this material, regardless of its penetration grade (50/70), is the one that is less capable of coping with cold climate conditions and is more prone to thermal cracking. When comparing binder A (40/60) to binder C (70/100), it was observed that the second one exhibited values of T_{cr} that were lower than those calculated for the first one. This is consistent with the relative penetration grades but is in contrast with T_g values (Table 2), which were found to be lower for binder A with respect to binder C. Such an outcome reveals that glass transition temperature alone should not be used for discriminating the low temperature properties of asphalt binders. On the contrary, the critical brittleness temperature introduced in the analysis of MTL test results seems to provide a reliable low temperature assessment of asphalt binders.

Table 4 Critical brittleness temperatures of asphalt binders

Binder	Strain rate [s^{-1}]	T_{cr} [°C]
A	0.0005	-25.2
	0.001	-19.9
B	0.0005	-13.8
	0.001	-13.4
C	0.0005	-22.9
	0.001	-20.1

5 Summary and conclusions

In this paper, a novel test procedure for the evaluation of low temperature failure properties of asphalt binders was presented, and its use was demonstrated by referring to an investigation performed on a set of selected materials.

After preliminary characterization, the considered asphalt binders were subjected to monotonic torsional loading (MTL) tests carried out with a Dynamic Shear Rheometer (DSR) at different temperatures and strain rates. The response of materials was quantitatively assessed by referring to the shear stress at failure, to a purposely defined brittleness index (I_B) and to a critical brittleness temperature (T_{cr}). The brittleness index was calculated as the ratio between actual and potential pseudo-strain energy densities determined according to the elastic-viscoelastic correspondence principle. This was applied to convert physical strains into pseudo-strains, thereby eliminating time effects from measured response. The critical brittleness temperature was associated to a threshold value of I_B that corresponds to a condition very close to purely brittle failure behaviour.

Results obtained from the investigation revealed that the proposed approach is effective in evaluating and discriminating the low temperature properties of the considered asphalt binders.

Specific conclusions drawn from the study can be summarized as follows:

- test specimens exhibited brittle-like or ductile-like failure mechanisms depending upon the combination of temperature and strain rate used for testing;
- shear stress at failure and I_B values increased with the decrease of temperature (or the increase of strain rate), leading to a temperature-dependent rank of the considered binders;
- the asphalt binder characterized by the highest glass transition temperature T_g showed the highest T_{cr} values, thus revealing a higher propensity to develop thermal cracking than the other considered binders;
- a univocal relationship between failure properties of materials and their glass transition temperatures could not be established.

This work represents the starting point in the development of the new methodology, so more research is certainly needed. In particular, the proposed protocol may need to be fine-tuned with respect to the selection of test geometry (gap and diameter), specimen preparation and conditioning prior to testing. A more extended investigation is also necessary to compare results with those of other standardized test methods and to assess test repeatability as well as reproducibility of test data. Finally, effects related to specific material properties, such as ageing and physical hardening, also deserve consideration in future works.

References

1. Haas RCG, Phang WA (1988) Relationships between mix characteristics and low temperature pavement cracking, J Assoc Asph Paving Technol 57:290–319.

2. Velasquez R, Bahia HU (2013) Critical factors affecting thermal cracking of asphalt pavements: towards a comprehensive specification, Road Mater Pavement Des 14(1): 187–200.

3. Zaumanis M, Poulikakos LD, Partl MN (2018) Performance-based design of asphalt mixtures and review of key parameters, Mater Des 141:185–201

4. Isacsson U, Zeng H, (1998) Cracking of asphalt at low temperature as related to bitumen rheology, J Mater Sci 33:2165–2170

5. Isacsson U, Zeng H (1997) Relationships between bitumen chemistry and low temperature behaviour of asphalt. Constr Build Mater 11:83–91

6. EN 12593 (2007) Bitumen and bituminous binders - Determination of the Fraass breaking point, European Committee for Standardization, CEN, Brussels

7. FEHRL (2006) BitVal - Analysis of available data for validation of bitumen tests. Report on Phase 1.
8. AASHTO T313 (2019) Standard method of test for determining the flexural creep stiffness of asphalt binder using the Bending Beam Rheometer (BBR). American Association of Highway State Officials, Washington, D.C.
9. AASHTO T314 (2012) Standard method of test for determining the fracture properties of asphalt binder in direct tension (DT). American Association of Highway State Officials, Washington, D.C.
10. AASHTO R49 (2009) Standard practice for determination of low-temperature performance grade (PG) of asphalt binders, American Association of Highway State Officials, Washington, D.C.
11. AASHTO M320 (2017) Standard Specification for Performance-Graded Asphalt Binder, American Association of Highway State Officials, Washington, D.C.
12. Ho S., Zanzotto L. (2005) The low temperature properties of conventional and modified asphalt binders evaluated by the failure energy and secant modulus from direct tension tests. Materials and Structures 38:137-143.
13. Airey, G.D., Choi, Y.K., Collop, A.C., Elliott, R. (2004) Rheological and fracture characteristics of low penetration grade bitumen. Road Materials and Pavement Design 5:107-131.
14. Lu X., Isacsson U. (2001) Effect of Binder Rheology on the Low-Temperature Cracking of Asphalt Mixtures. Road Materials and Pavement Design 2(1):29-47.
15. Mannan U. A., Islam M., Weldegiorgis M., Tarefder R. (2015) Experimental Investigation on Rheological Properties of Recycled Asphalt Pavement Mastics. Applied Rheology 25(2):1-9.
16. Brown E. R., Haddock J.E., Crawford C. (1996). Investigation of Stone Matrix Asphalt Mortars. Journal of the Transportation Research Board. 1530(1):95-102.
17. Cardone F., Frigio F., Ferrotti G., Canestrari F. (2015) Influence of mineral fillers on the rheological response of polymer-modified bitumens and mastics. Journal of Traffic and Transportation Engineering 2(6):373-381.
18. Cerni G, Cardone F, Colagrande S (2011) Low-temperature tensile behaviour of asphalt binders: Application of loading time–temperature–conditioning time superposition principle. Construction and Building Materials 25(4):2133-2145.
19. Baglieri O., Dalmazzo D.; Barazia M, Tabatabaee H.A, Bahia H.U. (2012) Influence of Physical Hardening on the Low-Temperature Properties of Bitumen and Asphalt Mixtures, In: PROCEDIA: SOCIAL & BEHAVIORAL SCIENCES, 504-513.
20. Santagata, E., Baglieri, O., Dalmazzo, D., Tsantilis, L. (2016) Experimental investigation on the combined effects of physical hardening and chemical ageing on low temperature properties of bituminous binders. RILEM Bookseries 11:631-641.
21. Marasteanu M, Ghosh D, Falchetto AC (2017) Testing protocol to obtain failure properties of asphalt binders at low temperature using creep compliance and stress-controlled strength test. Road Mater Pavement Des 18:352–367

22. Marasteanu MO, Zofka A, Turos M, Li X, Velasquez R, Li X, Buttlar W, Paulino G, Braham A, Dave E, Ojo J, Bahia H, Bausano CJ, Gallistel A, McGraw J (2007) Investigation of low temperature cracking in asphalt pavements: national pooled fund study 776. Final report, Minnesota Department of Transportation, St. Paul, MN
23. Lu X, Isacsson U, Ekblad J (2003) Influence of polymer modification on low temperature behaviour of bituminous binders and mixtures. Mater Struct 36: 652–656.
24. Moon KH, Marasteanu MO, Turos M (2013) Comparison of thermal stresses calculated from asphalt binder and asphalt mixture creep tests. J Mater Civ Eng 25(8):1059-1067
25. Lu X, Uhlback P, Soenen H (2017) Investigation of bitumen low temperature properties using a dynamic shear rheometer with 4 mm parallel plates. Int J Pavement Res Technol 10:15–22
26. Sui C, Farrar MJ, Harnsberger PM, Tuminello WH, Turner TF (2011) New low-temperature performance-grading method using 4-mm parallel plates on a Dynamic Shear Rheometer. Transp Res Record 2207:43-48
27. Farrar MJ, Sui C, Salmans S, Qin Q (2015) Determining the low temperature rheological properties of asphalt binder using a Dynamic Shear Rheometer (DSR). Technical White Paper, Fundamental Properties of Asphalts and Modified Asphalts III Product: FP 08. Western Research Institute, Laramie, WY
28. Farrar MJ, Kim SS, Pauli T, Planche JP (2016) An advanced low temperature rheological and fracture test method for bitumen purchase specifications and pavement performance prediction: 4-mm DSR/ABCD. In: 8th RILEM International Symposium on Testing and Characterization of Sustainable and Innovative Bituminous Materials. RILEM Bookseries, vol 11, Springer, pp. 25-36
29. AASHTO (2012) Draft standard method of test for determining the low temperature rheological properties of asphalt binder using a Dynamic Shear Rheometer (DSR). American Association of State Highway and Transportation Officials, Washington, D.C.
30. Schröter K, Hutcheson SA, Shi X, Mandanici A, Mckenna GB (2006) Dynamic shear modulus of glycerol: Corrections due to instrument compliance. J Chem Phys 125: 214507
31. Riccardi C, Falchetto AC, Wistuba MP, Losa M (2017) Comparison of DSR and BBR tests for determining the performance grade (PG) of asphalt binder at low temperature. In: 10th International Conference on the Bearing Capacity of Roads, Railways and Airfields (BCRRA). CRC Press, pp. 267–271
32. Wang D, Cannone Falchetto A, Alisov A, Schrader J, Riccardi C, Wisyuba MP (2019) An alternative experimental method for measuring the low temperature rheological properties of asphalt binder by using 4mm parallel plates on Dynamic Shear Rheometer. Transp Res Record 2672:427-438
33. Schapery RA (1984) Correspondence principles and a generalized J integral for large deformation and fracture analysis of viscoelastic media. Int J Fract 25:195–223

34. Santagata E, Baglieri O, Dalmazzo D, Tsantilis L (2009) Rheological and Chemical Investigation on the Damage and Healing Properties of Bituminous Binders. J Assoc Asph Paving Technol 78:567–596
35. Simnofske D., Mollenhauer K. (2019) Precision of Iatroscan Method for Assessment of SARA Compounds in Bitumen. RILEM 252-CMB 2018, RILEM 252-CMB-Symposium on Chemo Mechanical Characterization of Bituminous Materials 20: 162–167.
36. Dalmazzo, D., Jiménez Del Barco Carrión, A., Tsantilis, L., Lo Presti, D., Santagata, E. (2020) Non- petroleum- based binders for paving applications: Rheological and chemical investigation on ageing effects. Lecture Notes in Civil Engineering 48: 67-76.
37. Nellensteyn FJ (1924) The constitution of asphalt. J Inst Pet Technol 10:311–32529.
38. Lesueur D (2009) The colloidal structure of bitumen: consequences on the rheology and on the mechanisms of bitumen modification. Adv Colloid Interface Sci 145:42–82
39. Kriz P, Stastna J, Zanzotto L (2008) Physical aging in semi-crystalline asphalt binders. J Assoc Asph Paving Technol 77:795–826
40. Hesp SAM, Iliuta S, Shirokoff JW (2007) Reversible Aging in Asphalt Binders. Energy Fuels 21:1112–1121
41. Gaestel, C., Smadja, R. and Lamminan KA (1971) Contribution à la connaissence des propriétés des bitumes routiers. Rev générale des routes des aérodromes 466:85–97
42. Wang J, Wang T, Hou X, Xiao F (2019) Modelling of rheological and chemical properties of asphalt binder considering SARA fraction. Fuel 238:320–330
43. AASHTO T315 (2012) Standard method of test for determining the rheological properties of asphalt binder using a Dynamic Shear Rheometer (DSR). American Association of State Highway Transportation Officials, Washington, DC
44. Airey GD (2002) Use of Black Diagrams to Identify Inconsistencies in Rheological Data. Road Mater Pavement Des 3:403–424
45. Loebera L, Muller G, Morel J, et al (1998) Bitumen in colloid science: a chemical, structural and rheological approach. Fuel 77:1443–1450
46. Kriz P, Stastna J, Zanzotto L (2011) Glass transition and phase stability in asphalt binders. Road Mater Pavement Des 9:37–65
47. Anderson DA, Marasteanu MO (1999) Physical hardening of asphalt binders relative to their glass transition temperature. Transp Res Record 1661:27-34
48. Christensen DW, Anderson DA (1992) Interpretation of dynamic mechanical test data for paving grade asphalt. J Assoc Asph Pav Technol 61:67–116
49. Mackay ME, Halley P (1991) Technical Note: angular compliance error in force rebalance torque transducers. J Rheol 35:1609–1614
50. Wulpi DJ (1999) Understanding how components fail, 2nd ed. ASM International

51. University of Colorado Boulder (2016) Torsion of circular section. Introd to Aerosp Struct ASEN 3112 - Struct.